

PAPER • OPEN ACCESS

Mechanical and electrical properties of additively manufactured copper

To cite this article: J Rodriguez *et al* 2021 *IOP Conf. Ser.: Mater. Sci. Eng.* **1193** 012034

View the [article online](#) for updates and enhancements.

You may also like

- [Liquid crystal alignment in electro-responsive nanostructured thermosetting materials based on block copolymer dispersed liquid crystal](#)
A Tercjak, I Garcia and I Mondragon
- [Fermion mixing in an \$S_3\$ model with three Higgs doublets](#)
F González Canales, A Mondragón, M Mondragón et al.
- [\$S_3\$ flavour symmetry and the reactor mixing angle](#)
O Felix-Beltran, F Gonzalez Canales, A Mondragon et al.



The Electrochemical Society
Advancing solid state & electrochemical science & technology

242nd ECS Meeting

Oct 9 – 13, 2022 • Atlanta, GA, US

Abstract submission deadline: **April 8, 2022**

Connect. Engage. Champion. Empower. Accelerate.

MOVE SCIENCE FORWARD



Submit your abstract



Mechanical and electrical properties of additively manufactured copper

J Rodriguez^{1*}, J I Vicente², J C Ezeiza², A Zuriarrain², P J Arrazola³, X Badiola⁴, E Dominguez³ and D Soler³

¹ Industrial Engineering Master Student, Mondragon Unibertsitatea, Mondragon, Spain

² Engineering Department, Campus Goierrri – Mondragon Unibertsitatea, Mondragon, Spain

³ Manufacturing Department, Faculty of Engineering – Mondragon Unibertsitatea, Mondragon, Spain

⁴ Electronics and Computer Science department, Faculty of Engineering – Mondragon Unibertsitatea, Mondragon, Spain

*Corresponding author: jon.rodriquezc@alumni.mondragon.edu

Abstract: Additive Manufacturing (AM) has become the new paradigm of design and production strategies. While structural and functional materials are the most implemented ones, it is also possible to manufacture parts using precious metals, being copper one of the most interesting. Among AM technologies, the novel Atomic Diffusion Additive Manufacturing (ADAM) has recently included this material between available ones. ADAM is free from thermal and energetic issues caused by high reflectivity and conductivity of copper which other AM encounter. Therefore, it could be a great alternative to manufacture pure copper. In this work ADAM was used to fabricate pure copper specimens in order to measure electrical and mechanical properties. The influence of a machining post processes in strength and ductility is also discussed. Results are compared with wrought C1 1000 copper and published results of other AM technologies. Despite the newness of ADAM, significant improvement in surface roughness and comparable results in other properties was observed. However, further research shall be done to optimize the manufacturing parameters in order to increase the relative density value, as it was found to be significantly lower than in other AM technologies.

Keywords: Additive Manufacturing, ADAM, Copper, Conductivity, Mechanical, Machining.

1. Introduction

Additive Manufacturing (AM) technologies have been in constant development since the 1980's [1]. During this time, many AM technologies for metallic materials have been developed [2,3]. The novel feature of manufacturing 3D parts by adding thin layers of material allows production of complex functional parts directly from design avoiding the need of expensive tooling and conventional processing steps. Moreover, parts can be produced on demand, decreasing the lead time of obsolete replacement components and reducing the stock. Therefore, AM is becoming the new paradigm of design and production strategies.

A wide range of metallic materials can be processed by AM technologies. Although structural or functional materials such as steel, aluminium, titanium or nickel alloys are the most manufactured metals and the main research focus, precious metals as gold, silver or copper are also manufactured successfully.



Copper is known for its great conductivity and is widely used in many applications including high efficiency electric machines. Currently, Selective Laser Melting (SLM) [4] and Electron Beam Melting (EBM) [5] are the most developed AM technologies which work with copper [6]. Both technologies use focused energy beams to melt pre-alloyed metal powders forming small melt pools which rapidly solidify [7]. Its high conductivity property causes rapid heat dissipation and high local thermal gradients resulting in thermal issues such as layer curling, delamination, and finally in part failure [6]. Moreover, reflectivity of copper to conventional laser light is high, and therefore, greater laser output power is required in SLM compared to power used with other metals. The novel Atomic Diffusion Additive Manufacturing (ADAM) technology, which can manufacture pure copper parts since middle 2020, is free from reflectivity and conductivity issues during the manufacturing process, making it a great alternative to manufacture copper efficiently.

ADAM technology is based on three independent stages to manufacture as built functional parts: printing, washing and sintering. The first printing stage is very similar to the currently very developed and world widely used Fused Deposition Modelling (FDM) [8] technology. ADAM uses wire shaped raw material, which is composed of metal powder enclosed in a mix of wax and thermoplastic polymer matrix which works as a binder for the metallic particles [9]. The wire is extruded through a heated unit which softens the wax and at the end of the unit a nozzle is used to deposit the material in the build plate, and the same process is repeated layer by layer until the desired part is obtained.

Each layer consists of two deposition strategies (figure 1). Firstly, material is extruded following the shape of the part using a contour strategy, and secondly, the infill of the part is done to finish the layer. The infill can be done by creating a triangular lattice, which reduces part weight but not useful for functional parts, or by a zig zag solid infill strategy (figure 1 case), in which each layer is deposited perpendicularly with respect to the previous one.

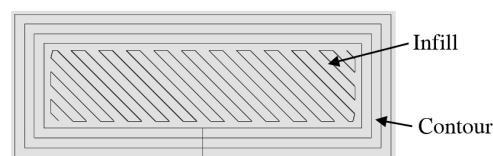


Figure 1. Deposition strategies.

If the part presents an overhang feature with 50° or smaller angle, a support structure printed in same metal as part is printed automatically. A ceramic material release layer is introduced between the part and support in order to facilitate the removal of the support structure in the final stage. In figure 2(a) an example of a designed part is shown containing a 48° overhang feature, and figure 2(b) shows the support structure. At the end of this stage, the obtained part is called green part.



Figure 2. Example of support structure. (a) Designed part. (b) Printed part.

The second step, the debinding or washing, consists on introducing the green part into a liquid solvent for a specific required time and fixed temperature to get rid of most of the wax binding material. The part after this stage, known as brown part, is very brittle and needs to be manipulated carefully.

The final step is the sintering. The brown parts are introduced into a furnace, in which a controlled flow of inert gas mix of argon and hydrogen fills the furnace chamber to protect the parts from oxidation, and they get a sintering cycle. This cycle is divided in two stages as it can be seen in figure 3(a). In the first step the remaining few wax and the thermoplastic polymer binder materials are burnt out. In the second one, the temperature is risen a bit more (always behind the melting point of the material), and due to diffusion bonding, all the metal powder particles are joined, getting as a result an almost fully dense and compact final part. The brown part is shrunk in size around 16% in this sintering stage, an example is shown in figure 3(b) and figure 3(c).

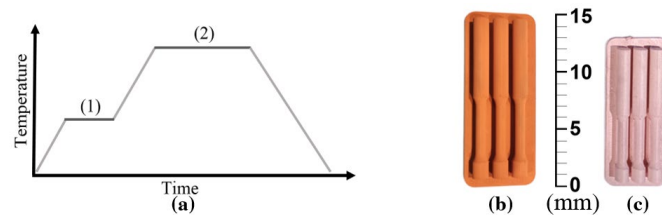


Figure 3. Sintering stage. (a) Sintering qualitative cycle. (b) Brown part example. (c) Sintered part example.

The objective of this article is to obtain the relative density, electrical conductivity, yield and tensile strength, maximum elongation, surface roughness and hardness of pure copper printed parts with ADAM technology, and compare them with ones found in previous research of SLM, EBM and wrought copper parts. Moreover, the effect of a machining post processing will also be analysed for the strength and ductility.

2. Methodology

In order to carry out mentioned analysis, standardised specimens were manufactured, and some tests performed. Metal X system developed by Markforged [10], which is based on ADAM technology, was used to manufacture these specimens. Such system consists of three different units: Metal X for the first extrusion step (figure 4(a)), the Wash-1 for the second debinding step (figure 4(b)) and the Sinter-1 for the last sintering step (figure 4(c)).



Figure 4. Metal X system. (a) Metal X. (b) Wash-1. (c) Sinter-1.

The exact distribution of the chemical components of the metal powder used in this study, commercialised by Markforged [11], is shown in table 1.

Table 1. Chemical components of the copper.

	Copper	Oxygen	Iron	Other
Amount (%)	99.8 min	0.05 max	0.05 max	bal

As for the parameter values in the first extrusion stage, the height of layer was set on 129 μm , a solid infill pattern was selected for all the specimens and the contour layer thickness of 1 mm in all specimen,

except for the machined tensile specimens which it was of 0.5 mm. For the washing, the solvent Opteon SF-79 was used. For the final sintering cycle, all the parameters were determined by the manufacturer.

2.1. Part density measurements

Density is one of the most important characteristics which has enormous influence in the final part properties. Therefore, it is essential to determine the overall density that ADAM technology can achieve.

There are three major methods to determine part density values: Archimedes method, micrograph of a cross section and X-ray scanning [12]. For this study the Archimedes method was found as most adequate. On the one hand, X-ray scanning requires a high computational cost for precise results. On the other hand, the micrograph study only determines the density value in a specific cross section. However, AM technologies tend to manufacture parts with heterogeneous microstructure and porosity distribution [13]. ADAM is not an exception as cavities were found heterogeneously distributed in the contour layer (figure 5). Therefore, the micrograph method is not accurate to correlate the cross-sectional density to overall density. Whereas, by Archimedes method, which is simple to apply and has high repeatability [12], full part density value were obtained.

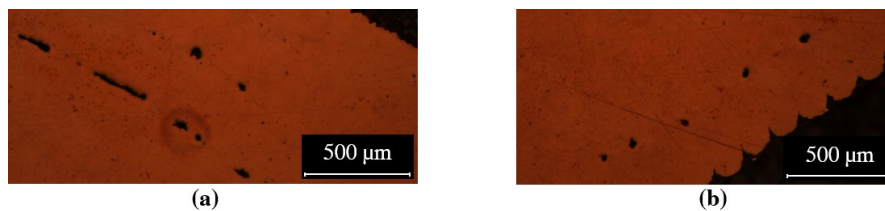


Figure 5. Different views relative to the deposition layers of cavities found in contour layer. (a) Parallel view. (b) Orthogonal view.

For such measurement, the Standard ASTM B962 [14] was followed. Part density (ρ_p) and relative density (RD) values were calculated by the equation (1), where ρ_w is the density of the distilled water, m_a is the mass of the dry part, m_f is the mass of the part while being immersed in water and ρ_c which is the theoretical real density of the prime material (8.96 g/cc) [11].

$$\rho_p = \frac{\rho_w \cdot m_a}{m_a - m_f} \rightarrow RD (\%) = \frac{\rho_p}{\rho_c} \cdot 100 \quad (1)$$

Six cubic samples of 20 mm³ were used for this study and each mass measurement was performed three times in order to obtain reliable results.

2.2. Electrical conductivity measurements

Recent articles have reported electrical conductivity values for copper using different measuring methods. Some were performed using induced Eddy currents, only getting superficial local electrical conductivity results [15,16]. Therefore, induced Eddy currents method does not directly measure resistivity, but rather it calculates surface conductivity and assume isotropic properties [17], which is not a reasonable assumption in additively manufactured parts.

To avoid such problems, electrical DC resistance testing was conducted based on the standard ASTM B193 [18]. Nine square base prism specimens of 2 mm x 2 mm x 25 mm were manufactured, six horizontally and three vertically, and all measurements were made using a four-wire DC Kelvin resistance measurement method with the microhmmeter CA 6255.

As resistance measurements R_t were carried out at room temperature t of 23°C, a correction factor α was used to get the corrected electrical resistance R_T for the reference temperature T of 20°C. With the corrected electrical resistance, the electrical resistivity ρ is calculated in $\mu\Omega \cdot \text{cm}$ by equation (2). Where R_T is the corrected electrical resistance in $\mu\Omega$, A is the cross-sectional area of the specimen in cm² and L is the length of the specimen in cm.

$$R_T = \frac{R_t}{1 + \alpha \cdot (t - T)} \rightarrow \rho = \frac{R_T \cdot A}{L} \quad (2)$$

The electrical resistivity value is then compared with the value of IACS (International Annealed Copper Standard). The reference value of 100% IACS is established in $17.241 \mu\Omega\cdot\text{cm}$ [19], being this the value of the annealed pure copper. This way a clearer view of the obtained results can be obtained.

2.3. Tensile tests

By these test the strength and ductility of the material were obtained. The specimens have been designed following the European Standard ISO 6892-1 [20]. Circular section test tubes with values shown in table 2 were chosen for this study, being L_t the total length of the specimen, L_c the parallel length, L_0 the gauge length, r the transition radius, d the diameter of the parallel length and D the diameter at grip.

Table 2. Most relevant measures of the tensile specimen.

	L_t	L_c	L_0	r	d	D
Measures (mm)	70	33	30	12	6	10

In order to get the machining post process influence, six extra samples were manufactured with an extra 1.6 mm in every diameter. Those specimens were then machined using a lathe, removing 0.8 mm from the surface and obtaining the standardised specimens.

The amount of material being removed was established in order to remove all the 0.5 mm contour layer, as it was found to be a more porous area than the core of the parts. Such porous area in the contour is previously shown in figure 5.

All specimens were manufactured in horizontal deposition strategy as shown in figure 3(c), which is the recommended by manufacturer to get the best mechanical properties. Nine tensile specimens were manufactured and tested overall, being three as built specimens and the other six machined ones. The tensile tests were carried out using the universal machine INSTRON 3369 and a self-supporting Macro extensometer was used to measure the strain. All the tensile tests were carried out with a strain rate of 3 mm/min in the elastic zone and 10 mm/min in the plastic zone.

2.4. Surface roughness measurements

In order to analyse the surface roughness in different plane angles, four specimens were manufactured as shown in figure 6(a). With them the following planes were measured: 0° , 30° , 45° , 60° , 90° , 130° and 180° . Figure 6(b) is for the visual understanding of each surface plane. The surfaces with an angle of over 130° require a support structure which must be removed after sintering. Three measurements were made in each plane angle. R_a , R_z and R_{max} were measured using a Hommel Tester T500.

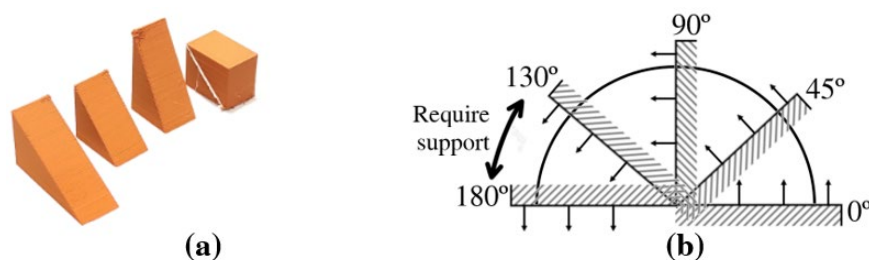


Figure 6. Surface roughness. (a) Specimens. (b) Visual explanation for the surface angles.

2.5. Hardness measurements

As roughness measurements are non-destructive, Vickers surface hardness values were obtained using the figure 6(a) specimens to analyse different plane angles. The objective surfaces were sanded progressively, using first $240 \mu\text{m}$, then $600 \mu\text{m}$, afterwards $800 \mu\text{m}$ and finally $1200 \mu\text{m}$ sandpaper. A Zwick Vickers hardness tester was used applying 1 Kg for 10 seconds. Five measurements were made in all plane angles.

3. Results

All results of the described tests and measurements are given in table 3 as well as SLM, EBM and wrought reference values of pure copper found in the literature. AM given results are the arithmetic mean of performed tests and the corresponding standard deviation.

For the wrought values, C1 1000 copper was taken as the reference material as it is commonly used in electrical applications, and the values are given with upper and lower thresholds. The range is due to the temper type and the section thickness of the mill product [21].

In the case of SLM and EBM values, process input parameters are defined in given references. N.A. are for values which were not found in the literature.

Table 3. All results and comparison with other technology values.

		ADAM	SLM [22]	EBM [15]	WROUGHT [21]
Relative density (%)		94.51±0.41	99.1±0.5 ^a	99.5 ^a	100
Electrical conductivity (%IACS)		86.11±6.92 ^b	88±2 [23]	100 ^c	100
Yield Strength (MPa)	As built	45.67±2.52	187±5.3	78.1±0.9	69 - 365
	Machined	61.33±10.03	N.A.	N.A.	N.A.
Tensile Strength (MPa)	As built	205.87±0.07	248±8.5	177±3.3	221 - 455
	Machined	182.19±11.1	N.A.	N.A.	N.A.
Maximum elongation (%)	As built	37.07±4.1	9.2±1.75	59.3±7.5	4 - 55
	Machined	31.36±10.08	N.A.	N.A.	N.A.
Surface roughness (µm)	<i>Ra</i>	3.3±0.2 ^d	12.72±4.5	N.A.	N.A.
	<i>Rz</i>	18.5±1.9 ^d	N.A.	N.A.	N.A.
	<i>Rmax</i>	23.9±3.5 ^d	N.A.	N.A.	N.A.
Vickers hardness (HV)	Surface values	37.6±5.5	85±4.2	57.8±1.55	40 - 130

^a Obtained by micrograph of a cross section measurement strategy.

^b Results for horizontal specimens only.

^c Superficial and local results. Induced Eddy currents measuring method.

^d Values for the plane angle of 0°. Best values measured.

4. Discussion

Due to its high influence in the mechanical and electrical properties, the first and most important result to be analysed is the relative density (RD). While in the more developed AM technologies such as SLM and EBM the manufacturing parameters are already optimized to achieve a near 100% density values, in novel ADAM are below 95%. Future research is required to optimize manufacturing stages (printing, washing and sintering) in order to get rid of cavities similar to those shown in figure 5 and improve its relative density.

Regarding the electrical conductivity, high values are currently achieved in ADAM technology. Moreover, it is believed that an improvement in RD will directly improve the conductivity value as it is well known that cavities cause an electrical conductivity reduction [24]. Vertically manufactured specimens were found to have 23% worse conductivity than horizontally built ones, suggesting a heterogeneous microstructure of the parts.

Highest tensile strength and lowest maximum elongation values were found in SLM due to the high cooling rates this technology has in the manufacturing process [22]. Such high temperature gradients cause small grain size microstructure which explain such results. In case of the EBM study, a high powder bed temperature had been set obtaining bigger grain size microstructure [15], resulting in lowest tensile strength and highest maximum elongation values. As for ADAM, the small temperature gradients in the sintering cycle is believed to cause a big grain size microstructure and more ductile properties than SLM (future microstructure analysis should be done to prove the expected big grain sizes). Having the sintering thermal cycle included in the technology allows to obtain a variety of microstructure depending on the programmed cycle, being able to adjust the final part properties to application

requirements.

Surface roughness values of ADAM in table 3 corresponds to those measured in the plane angle of 0° , the best achieved. Worse values were measured in all the plane angles which are shown in figure 7. Although better results than in SLM were achieved, the values measured are far from not requiring a surface post-processing operation as machining in the functional surfaces.

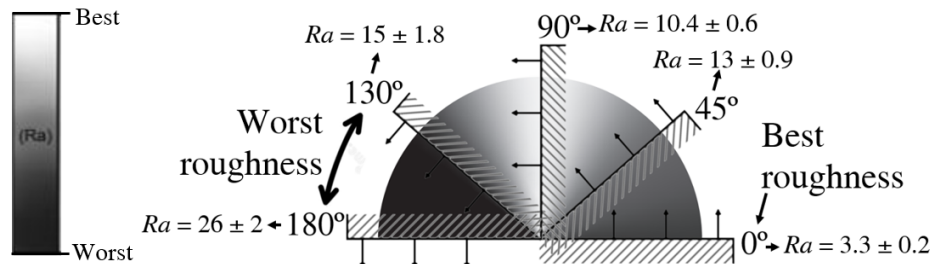


Figure 7. Results of surface roughness.

Two main factors could explain the Vickers hardness results in AM. On the one hand, the smaller the grain size, the higher the hardness. That's why SLM achieves the highest values. On the other hand, the presence of cavities in contour layers yields to lower hardness. The lowest hardness value obtained by ADAM could be explained by the cavities found near the surface as shown in figure 5 and the supposed big grain size.

Finally, concerning the machining influence in the tensile tests, although higher values in strength and elongation were expected for machined specimens compared to as built ones, machined parts showed worse mechanical properties. The reasons of such results were found to be (i) the poor machining quality of the parts, not obtaining a good surface roughness with little cracks in it, and (ii) the removal of the whole contour layer. Both reasons facilitated crack formation and its propagation causing premature failure in the specimens. The poor machining quality is also reflected in the big standard deviation obtained in both strengths and maximum elongations of the machined tests. This suggest that shown values are not representative. Therefore, further tests should be performed to drawn valuable conclusions.

5. Conclusions

Pure copper specimens were successfully manufactured by ADAM technology and measurements were carried out to obtain the mechanical and electrical properties.

Despite being a novel technology, currently obtained mechanical and electrical properties were comparable to those obtained by SLM and EBM. Being the best technology considering surface roughness. However, electrical conductivity and hardness were measured with lowest values.

Relative density value was found to be significantly lower than in other AM technologies. Therefore, further research shall be done to optimize the manufacturing parameters in order to increase its value. Mechanical and electrical properties are believed to increase with a relative density improvement. Furthermore, taking into account that sintering is included in the process, modifying the sintering cycle, ADAM can achieve specific microstructure and properties for required applications.

Evidence of anisotropy of the part was measured by the 23% difference in electrical conductivity.

Results of machining influence on mechanical properties cannot be considered as definitive because of the poor machining quality achieved in the tested specimens.

Acknowledgements

The authors would like to thank the Basque Government for the financial support to the Tknika 025_020 project.

References

- [1] Wong K V and Hernandez A 2012 A Review of Additive Manufacturing *ISRN Mech Eng* **2012** pp 1-10
- [2] Zhang Y, et al 2018 Additive Manufacturing of Metallic Materials: A Review *Journal of Materials Engineering and Performance* **27** pp 1-13
- [3] Frazier W E 2014 Metal additive manufacturing: A review *Materials Engineering and Performance* **23** pp 1917–1928
- [4] Yap C Y, Chua C K, Dong Z L, Liu Z H, Zhang D Q, Loh L E and Sing S L 2015 Review of selective laser melting: Materials and applications *Applied Physics Review* **2** (4) p 041101
- [5] Körner C 2016 Additive manufacturing of metallic components by selective electron beam melting - A review *International Materials Reviews* **61** pp 361-377
- [6] Tran T Q, et al 2019 3D printing of highly pure copper *Metals* **9** (7) p 756
- [7] Murr L E, et al 2012 Metal Fabrication by Additive Manufacturing Using Laser and Electron Beam Melting Technologies *Material Science and Technology* **28** (1) pp 1–14
- [8] Gebisa A W and Lemu H G 2018 Investigating effects of Fused-deposition modeling (FDM) processing parameters on flexural properties of ULTEM 9085 using designed experiment *Materials* **11** (4) p 500
- [9] Galati M and Minetola P 2019 Analysis of density, roughness, and accuracy of the atomic diffusion additive manufacturing (ADAM) process for metal parts *Materials* **12** (24) p 4122
- [10] Markforged Web Page (<https://markforged.com/>) accessed 20 April 2021
- [11] Markforged 2020 *Material Datasheet Copper* (<http://static.markforged.com/downloads/copper-data-sheet.pdf>) accessed 20 April 2021
- [12] Spierings A B, Schneider M and Eggenberger R 2011 Comparison of density measurement techniques for additive manufactured metallic parts *Rapid Prototyping* **17** (5) pp 380–386
- [13] Kok Y, et al 2018 Anisotropy and heterogeneity of microstructure and mechanical properties in metal additive manufacturing: A critical review *Materials and Design* **139** pp 565–586
- [14] ASTM B962-8 2008 Standard test methods for density of compacted or sintered powder metallurgy (PM) products using Archimedes' principle *ASTM International*
- [15] Guschlbauer R, Momeni S, Osmanlic F and Körner C 2018 Process development of 99.95% pure copper processed via selective electron beam melting and its mechanical and physical properties *Materials Characterization* **143** pp 163–170
- [16] Frigola P, et al 2014 Fabricating Copper Components with Electron Beam Melting *Advanced Materials and Processes* **172** (7) pp 20-24
- [17] Silbernagel C, Gargalis L, Ashcroft I, Hague R, Galea M and Dickens P 2019 Electrical resistivity of pure copper processed by medium-powered laser powder bed fusion additive manufacturing for use in electromagnetic applications *Additive Manufacturing* **29** p 100831
- [18] ASTM B193-20 2020 Standard test method for resistivity of electrical conductor materials *ASTM International*
- [19] European Copper Institute 2020 Copper as electrical conductive material with above standard performance properties (<https://conductivity-app.org/>) accessed 20 April 2021
- [20] ISO 6892-1 2020 Metallic materials - Tensile testing - Part 1: Test Method at Ambient Temperature *International Organization for Standardization*
- [21] Davis J R 2001 *Copper and Copper Alloys* (ASM Internationals)
- [22] Yan X, et al. 2020 Microstructure and mechanical properties of pure copper manufactured by selective laser melting *Materials Science and Engineering: A* **789** p 139615
- [23] Jadhav S D, Dadbakhsh S, Goossens L, Kruth J P, Van Humbeeck J and Vanmeensel K 2019 Influence of selective laser melting process parameters on texture evolution in pure copper *Journal of Materials Processing Technology* **270** pp 47–58
- [24] Singh G, Singh S, Singh J and Pandey P M 2020 Parameters effect on electrical conductivity of copper fabricated by rapid manufacturing *Materials and Manufacturing Processes* **35** (15) pp 1769–1780